Progress In Electromagnetics Research C, Vol. 97, 109–121, 2019

Both Worst Case and Outage Constrained Robust Design for MIMO Wiretap Wireless Sensor Networks

Feng Zhou[1, 3, *], Rugang Wang[1, 2], and Jinhong Bian[1, 3]

Abstract—In this paper, we consider a MIMO wiretap system in wireless sensor networks (WSNs), where the confidential signal sent to the legitimate receive (Bob) may be eavesdropped by the eavesdropper (Eve). Assuming that only partial channel state information (CSI) can be obtained by the transmitter, we consider both worst case (WC) and outage-constrained (OC) robust secrecy optimizations. To solve the WC design, we propose to linearize these logarithmic determinant terms. After linearization, we tackle the CSI uncertainty using the Nemirovski lemma. Then, an alternating optimization (AO) algorithm is proposed to solve the reformulated problem. On the other hand, to solve the OC design, we transform the probabilistic constraint into safe and tractable reformulation by the Bernstein-type inequality (BTI) and large deviation inequality (LDI), and an AO algorithm is proposed. Numerical results are provided to demonstrate the performance of the proposed scheme.

1. INTRODUCTION

Wireless sensor networks (WSNs) are considered as a promising technique with numerous applications such as data acquisition, location monitoring, and node control [1, 2]. However, secure transmission has been seen as an important problem for WSN due to the openness of wireless channel [3, 4]. The physical layer security (PLS) technique, which exploits the characteristics of wireless channels, has been proved as an effective method to improve the security in wireless networks [5].

The design of transmit precoding or beamforming in multiple-input multiple-output (MIMO) wiretap channel is a typical non-convex problem [6, 7]. To solve this problem, various methods have been proposed in [8–13]. In [8], the authors proposed a transmit precoding design based on alternating optimization (AO). In [9], the authors proposed a method based on matrix generalized singular value decomposition (GSVD). In [10], the authors proposed an iterative custom-made method. In [11], the authors proposed an inexact block coordinate descent (IBCD) method to design information signal and energy signal in a secrecy MIMO system with energy harvesting (EH). Recently, the minorization-maximization (MM) based method has aroused new attention to design the precoding in MIMO wiretap channels [12, 13].

However, due to the existence of channel estimation and feedback errors, it is difficult to obtain perfect channel state information (CSI). Robust design has been widely investigated to handle this obstacle. Commonly, there are two kinds of robust design in wiretap channel, e.g., the worst case (WC) secrecy design and outage constraint (OC) secrecy design.

Specifically, the worst case robust optimizing problem was investigated in [14–18]. The technique to tackle the bounded CSI uncertainty in these works mostly involved the S-Procedure. However, for a MIMO wiretap channel, the S-Procedure is not directly workable since the secrecy rate expression

Received 28 September 2019, Accepted 19 November 2019, Scheduled 4 December 2019
* Corresponding author: Feng Zhou (zfycit@ycit.edu.cn).
[1] School of Information Technology, Yancheng Institute of Technology, Yancheng 224051, China. [2] Key Laboratory of Underwater Acoustic Signal Processing, Ministry of Education, Southeast University, Nanjing 210096, China. [3] Research Center of Photoelectric Technology, Yancheng Institute of Technology, Yancheng 224051, China.

consists of several logarithmic determinant (log-det) terms, not the matrix trace formulation as in the multiple-input single-output (MISO) channel. To overcome this obstacle, log-det is commonly approximated as a trace by first order Taylor series expansion [14–16]. However, at high SNR region, the difference between the actual value and this approximation is huge [17]. In [18], the authors proposed an epigraph reformulation to handle the CSI uncertainty without considering artificial noise (AN).

On the other hand, the outage constraint design has been investigated in [19–23]. In [19], the authors proposed an AO method to achieve a safe approximation for the secrecy outage design. In [20], the authors proposed a successive convex approximation (SCA) based method to maximize the outage secrecy rate. In [21], the authors proposed an SCA method to maximize the harvested energy at the energy receiver subject to the outage secrecy rate constraint. Recently in [22] and [23], the authors proposed AO based methods to maximize the outage secrecy rate in MIMO channel without and with considering AN, respectively.

Motivated by these observations, in this paper, we investigate the bounded and probabilistic CSI uncertainties constraint robust designs, respectively. Specifically, considering both imperfect Bob's and Eve's CSIs, we aim to optimize the transmit precoding matrix and AN covariance. We propose to linearize these log-det terms and utilize epigraph reformulation to deal with CSI uncertainties. Then, an AO algorithm is proposed to solve the reformulated problem. For the outage-constraint design, we transform the probabilistic constraint into tractable reformulation by Bernstein-type inequality (BTI) and large deviation inequality (LDI), to achieve better performance and lower complexity, respectively. Finally, numerical results demonstrate the performance of the proposed scheme.

The rest of this paper is organized as follows. The system model and problem statement are given in Section 2. Section 3 investigates the worst case secrecy design. Section 4 investigates the worst case secrecy design. Simulation results are provided in Section 5. Section 6 concludes this paper.

Notations: Throughout this paper, boldface lowercase and uppercase letters denote vectors and matrices, respectively. The conjugate, transpose, conjugate transpose, trace, and rank of matrix $\mathbf{A}$ are denoted as $\mathbf{A}^\dagger$, $\mathbf{A}^T$, $\mathbf{A}^H$, $\mathrm{Tr}(\mathbf{A})$, and $\mathrm{rank}(\mathbf{A})$, respectively. $\mathbf{a} = \mathrm{vec}(\mathbf{A})$ indicates to stack the columns of matrix $\mathbf{A}$ into a vector $\mathbf{a}$. $\mathbb{H}_+^N$ denotes the set of all $N \times N$ Hermitian positive semi-definite matrices. $\mathbf{A} \succeq \mathbf{0}$ indicates that $\mathbf{A}$ is a positive semi-definite matrix. $|\cdot|$ and $\|\mathbf{a}\|$ denote the absolute value and Euclidean norm of vector $\mathbf{a}$, respectively. $\otimes$ denotes the Kronecker product. $\mathbf{D}(\mathbf{a})$ represents a diagonal matrix with $\mathbf{a}$ on the main diagonal. $\mathbf{I}$ is an identity matrix with proper dimension. $\lambda_{\max}(\mathbf{A}, \mathbf{B})$ denotes the largest generalized eigenvalue of matrices $\mathbf{A}$ and $\mathbf{B}$. $\mathrm{Re}\{a\}$ denotes the real part of a complex variable a. $\mathcal{CN}(\mathbf{0}, \mathbf{I})$ denotes a circularly symmetric complex Gaussian random vector with mean $\mathbf{0}$ and covariance $\mathbf{I}$. $[x]^+$ indicates $\max(0, x)$, and $\mathbb{E}[\cdot]$ stands for the statistical expectation.

2. SYSTEM MODEL AND PROBLEM STATEMENT

2.1. Problem Statement

Let us consider a MIMO wiretap system, which consists of one transmitter (T), one legitimate receiver (Bob), and an eavesdropper (Eve), as shown in Fig. 1. It is assumed that the T, Bob, and Eve are equipped with N_t, N_b, and N_e antennas, respectively. The channel matrices between T and Bob, and between T and Eve are denoted as $\mathbf{H} \in \mathbb{C}^{N_b \times N_t}$ and $\mathbf{G} \in \mathbb{C}^{N_e \times N_t}$, respectively.

In this paper, we assume that only imperfect Bob's and Eve's CSIs can be obtained. The bounded CSI uncertainties are modeled as

$$\mathcal{H} = \left\{ \mathbf{H} \,\middle|\, \mathbf{H} = \bar{\mathbf{H}} + \Delta\mathbf{H},\ \|\Delta\mathbf{H}\| \le \chi_H \right\}, \tag{1a}$$

$$\mathcal{G} = \left\{ \mathbf{G} \,\middle|\, \mathbf{G} = \bar{\mathbf{G}} + \Delta\mathbf{G},\ \|\Delta\mathbf{G}\| \le \chi_G \right\}, \tag{1b}$$

where $\bar{\mathbf{H}}$ and $\bar{\mathbf{G}}$ denote the estimates of $\mathbf{H}$ and $\mathbf{G}$, respectively; $\Delta\mathbf{H}$ and $\Delta\mathbf{G}$ are their respective channel uncertainties; χ_H and χ_G denote the respective sizes of the bounded channel uncertainties region.

Accordingly, the worst case secrecy rate can be expressed as

$$R_{\text{worst}} = \min_{\forall\,\mathbf{H} \in \mathcal{H},\, \forall\,\mathbf{G} \in \mathcal{G}} C_b\left(\mathbf{W}, \mathbf{\Sigma}\right) - C_e\left(\mathbf{W}, \mathbf{\Sigma}\right), \tag{2}$$

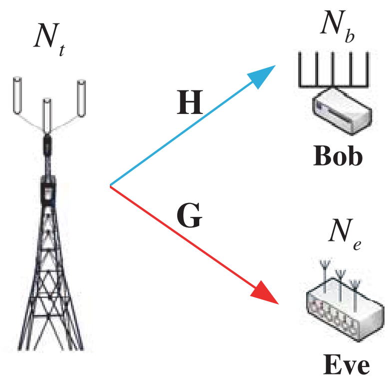

Figure 1. The MIMO wiretap system model.

where C_b and C_e denote the mutual information at Bob and Eve, respectively, and are given by

$$C_b(\mathbf{W},\mathbf{\Sigma}) \triangleq \ln\left|\mathbf{I}+\mathbf{H}\mathbf{W}\mathbf{W}^H\mathbf{H}^H\left(\sigma_b^2\mathbf{I}+\mathbf{H}\mathbf{\Sigma}\mathbf{H}^H\right)^{-1}\right|, \tag{3a}$$

$$C_e(\mathbf{W},\mathbf{\Sigma}) \triangleq \ln\left|\mathbf{I}+\mathbf{G}\mathbf{W}\mathbf{W}^H\mathbf{G}^H\left(\sigma_e^2\mathbf{I}+\mathbf{G}\mathbf{\Sigma}\mathbf{G}^H\right)^{-1}\right|. \tag{3b}$$

On the other hand, for the outage constraint design, the CSI uncertainties are modeled as follows

$$\mathcal{H}=\left\{\mathbf{H}\left|\mathbf{H}=\bar{\mathbf{H}}+\Delta\mathbf{H},\ \mathrm{vec}(\Delta\mathbf{H})\sim\mathcal{CN}(\mathbf{0},\mathbf{C}_H)\right.\right\}, \tag{4a}$$

$$\mathcal{G}=\left\{\mathbf{G}\left|\mathbf{G}=\bar{\mathbf{G}}+\Delta\mathbf{G},\ \mathrm{vec}(\Delta\mathbf{G})\sim\mathcal{CN}(\mathbf{0},\mathbf{C}_G)\right.\right\}, \tag{4b}$$

where $\Delta\mathbf{H}$ and $\Delta\mathbf{G}$ denote the channel uncertainties, respectively; $\mathbf{C}_H$ and $\mathbf{C}_G$ denote the covariances, respectively.

Accordingly, the secrecy outage probability can be expressed as

$$\Pr\left\{\min_{\forall\mathbf{H}\in\mathcal{H},\forall\mathbf{G}\in\mathcal{G}} C_b(\mathbf{W},\mathbf{\Sigma})-C_e(\mathbf{W},\mathbf{\Sigma})\geq R_{out}\right\}\geq 1-\rho, \tag{5}$$

where ρ is the secrecy outage probability, e.g., the chance of the achievable secrecy rate R falling below the target rate R_s due to CSI uncertainty.

2.2. Problem Statement

In this paper, we investigate the joint precoding and AN design to maximize the worst case secrecy rate and outage secrecy rate, respectively. Mathematically, the two problems can be formulated as

$$\begin{aligned}\mathrm{P1}: \max_{\mathbf{W},\mathbf{\Sigma}\succeq\mathbf{0}} &\left[\min_{\|\Delta\mathbf{H}\|_F\leq\chi_H} \ln\left|\mathbf{I}+\mathbf{H}\mathbf{W}\mathbf{W}^H\mathbf{H}^H\left(\sigma_b^2\mathbf{I}+\mathbf{H}\mathbf{\Sigma}\mathbf{H}^H\right)^{-1}\right|\right.\\ &\left.-\max_{\|\Delta\mathbf{G}\|_F\leq\chi_G} \ln\left|\mathbf{I}+\mathbf{G}\mathbf{W}\mathbf{W}^H\mathbf{G}^H\left(\sigma_e^2\mathbf{I}+\mathbf{G}\mathbf{\Sigma}\mathbf{G}^H\right)^{-1}\right|\right],\end{aligned} \tag{6a}$$

$$\text{s.t.}\quad \mathrm{Tr}\left(\mathbf{W}\mathbf{W}^H+\mathbf{\Sigma}\right)\leq P_s, \tag{6b}$$

$$\mathrm{P2}: \max_{\mathbf{W},\mathbf{\Sigma}\succeq\mathbf{0}}\quad R_{out} \tag{7a}$$

$$\text{s.t. }\Pr\left\{\min_{\forall\mathbf{H}\in\mathcal{H},\forall\mathbf{G}\in\mathcal{H}} C_b(\mathbf{W},\mathbf{\Sigma})-C_e(\mathbf{W},\mathbf{\Sigma})\geq R_{out}\right\}\geq 1-\rho, \tag{7b}$$

$$\text{(6b)}, \tag{7c}$$

where P_s is the maximum achievable power for the transmitter.

3. WORST CASE SECRECY DESIGN

P1 is highly non-convex due to maximize the difference of several log-det functions in the CSI uncertainty region. In this section, we will propose en effective method to linearize these log-det terms and handle the CSI uncertainty.

Firstly, we introduce the following Lemma.

Lemma 1 [11]: Define an m by m matrix function,

$$\mathbf{\Xi}(\mathbf{U},\mathbf{V}) \triangleq \mathbf{U}^H\mathbf{N}\mathbf{U} + \left(\mathbf{I}-\mathbf{U}^H\mathbf{M}\mathbf{V}\right)\left(\mathbf{I}-\mathbf{U}^H\mathbf{M}\mathbf{V}\right)^H,$$

where $\mathbf{N}$ is any positive definite matrix. Then, the following three equations hold true.

Equation (1): For any positive definite matrix $\mathbf{S}\in\mathbb{C}^{m\times m}$, we have

$$\mathbf{S}^{-1} = \arg\max_{\mathbf{T}\succ\mathbf{0}} \ln|\mathbf{T}| - \mathrm{Tr}(\mathbf{T}\mathbf{S}),$$

and

$$-\ln|\mathbf{S}| = \arg\max_{\mathbf{T}\succ\mathbf{0}} \ln|\mathbf{T}| - \mathrm{Tr}(\mathbf{T}\mathbf{S}) + m.$$

Equation (2): For any positive definite matrix $\mathbf{T}$, we have

$$\tilde{\mathbf{U}} \triangleq \arg\min_{\mathbf{U}} \mathrm{Tr}(\mathbf{T}\mathbf{\Xi}(\mathbf{U},\mathbf{V})) = \left(\mathbf{N}+\mathbf{M}\mathbf{V}\mathbf{V}^H\mathbf{M}^H\right)^{-1}\mathbf{M}\mathbf{V},$$

and

$$\mathbf{\Xi}\left(\tilde{\mathbf{U}},\mathbf{V}\right) = \mathbf{I}-\tilde{\mathbf{U}}^H\mathbf{M}\mathbf{V} = \left(\mathbf{I}+\mathbf{V}^H\mathbf{M}^H\mathbf{N}^{-1}\mathbf{M}\mathbf{V}\right)^{-1}.$$

Equation (3): We have

$$\ln\left|\mathbf{I}+\mathbf{M}\mathbf{V}\mathbf{V}^H\mathbf{M}^H\mathbf{N}^{-1}\right| = \arg\max_{\mathbf{T}\succ\mathbf{0},\mathbf{U}} \ln|\mathbf{T}| - \mathrm{Tr}(\mathbf{T}\mathbf{\Xi}) + m.$$

Equations (1) and (2) can be proven by the first-order optimality condition, while Equation (3) directly follows from Equations (1) and (2) and the identity $\ln|\mathbf{I}+\mathbf{A}\mathbf{B}| = \ln|\mathbf{I}+\mathbf{B}\mathbf{A}|$.

Eq. (6) is hard to handle due to the coupled variables and non-convex objective and constraints. In the following, we will decouple Eq. (6) based on these above equations.

To utilize the above equations, we denote $\mathbf{\Sigma}=\mathbf{Q}\mathbf{Q}^H$ and rewrite R_s as

$$\begin{aligned} R_s = & \underbrace{\ln\left|\mathbf{I}+\sigma_b^{-2}\mathbf{H}\mathbf{W}\mathbf{W}^H\mathbf{H}^H\left(\mathbf{I}+\sigma_b^{-2}\mathbf{H}\mathbf{Q}\mathbf{Q}^H\mathbf{H}^H\right)^{-1}\right|}_{f_1} + \underbrace{\ln\left|\mathbf{I}+\sigma_e^{-2}\mathbf{G}\mathbf{Q}\mathbf{Q}^H\mathbf{G}^H\right|}_{f_2} \\ & + \ln\left|\sigma_e^2\mathbf{I}\right| - \underbrace{\ln\left|\sigma_e^2\mathbf{I}+\mathbf{G}\mathbf{W}\mathbf{W}^H\mathbf{G}^H+\mathbf{G}\mathbf{Q}\mathbf{Q}^H\mathbf{G}^H\right|}_{f_3}, \end{aligned} \tag{8}$$

where

$$f_1 = \max_{\mathbf{\Psi}_1\succ\mathbf{0},\mathbf{U}} \ln|\mathbf{\Psi}_1| - \mathrm{Tr}(\mathbf{\Psi}_1\mathbf{\Xi}_1(\mathbf{U},\mathbf{W},\mathbf{Q})) + N_d, \tag{9a}$$

$$f_2 = \max_{\mathbf{\Psi}_2\succ\mathbf{0},\mathbf{V}} \ln|\mathbf{\Psi}_2| - \mathrm{Tr}(\mathbf{\Psi}_2\mathbf{\Xi}_2(\mathbf{V},\mathbf{Q})) + N_T, \tag{9b}$$

$$f_3 = \max_{\mathbf{\Psi}_3\succ\mathbf{0}} \ln|\mathbf{\Psi}_3| + N_E - \mathrm{Tr}\left(\mathbf{\Psi}_3\left(\sigma_e^2\mathbf{I}+\mathbf{G}\mathbf{W}\mathbf{W}^H\mathbf{G}^H+\mathbf{G}\mathbf{Q}\mathbf{Q}^H\mathbf{G}^H\right)\right). \tag{9c}$$

Furthermore, the matrix functions $\mathbf{\Xi}_1$ and $\mathbf{\Xi}_2$ are as follows

$$\mathbf{\Xi}_1(\mathbf{U},\mathbf{W},\mathbf{Q}) \triangleq \mathbf{U}^H\left(\mathbf{I}+\sigma_b^{-2}\mathbf{H}\mathbf{Q}\mathbf{Q}^H\mathbf{H}^H\right)\mathbf{U} + \left(\mathbf{I}-\sigma_b^{-1}\mathbf{U}^H\mathbf{H}\mathbf{W}\right)\left(\mathbf{I}-\sigma_b^{-1}\mathbf{U}^H\mathbf{H}\mathbf{W}\right)^H, \tag{10a}$$

$$\mathbf{\Xi}_2(\mathbf{V},\mathbf{Q}) \triangleq \sigma_e^{-2}\mathbf{V}^H\mathbf{V} + \left(\mathbf{I}-\sigma_e^{-1}\mathbf{V}^H\mathbf{G}\mathbf{Q}\right)\left(\mathbf{I}-\sigma_e^{-1}\mathbf{V}^H\mathbf{G}\mathbf{Q}\right)^H. \tag{10b}$$

Based on the above relationships, Eq. (6) can be rewritten as

$$\max_{\substack{\boldsymbol{\Psi}_1\succ\mathbf{0},\boldsymbol{\Psi}_2\succ\mathbf{0},\\ \boldsymbol{\Psi}_3\succ\mathbf{0},\mathbf{U},\\ \mathbf{V},\mathbf{W},\mathbf{Q}}} \ln|\boldsymbol{\Psi}_1| - \mathrm{Tr}\left(\boldsymbol{\Psi}_1\mathbf{U}^H\mathbf{U}\right) - a - b + \ln|\boldsymbol{\Psi}_2| - \sigma_e^{-2}\mathrm{Tr}\left(\boldsymbol{\Psi}_2\mathbf{V}^H\mathbf{V}\right) - c \tag{11a}$$

$$+\ln|\boldsymbol{\Psi}_3| - \sigma_e^2\mathrm{Tr}\left(\boldsymbol{\Psi}_3\right) - d - e,$$

$$\text{s.t. } \mathrm{Tr}\left(\boldsymbol{\Psi}_1\left(\mathbf{I}-\sigma_b^{-1}\mathbf{U}^H\mathbf{H}\mathbf{W}\right)\left(\mathbf{I}-\sigma_b^{-1}\mathbf{U}^H\mathbf{H}\mathbf{W}\right)^H\right) \le a, \tag{11b}$$

$$\mathrm{Tr}\left(\boldsymbol{\Psi}_1\mathbf{U}^H\mathbf{H}\mathbf{Q}\mathbf{Q}^H\mathbf{H}^H\mathbf{U}\right) \le \sigma_b^2 b, \tag{11c}$$

$$\mathrm{Tr}\left(\boldsymbol{\Psi}_2\left(\mathbf{I}-\sigma_e^{-1}\mathbf{V}^H\mathbf{G}\mathbf{Q}\right)\left(\mathbf{I}-\sigma_e^{-1}\mathbf{V}^H\mathbf{G}\mathbf{Q}\right)^H\right) \le c, \tag{11d}$$

$$\mathrm{Tr}\left(\boldsymbol{\Psi}_3\mathbf{G}\mathbf{W}\mathbf{W}^H\mathbf{G}^H\right) \le d, \tag{11e}$$

$$\mathrm{Tr}\left(\boldsymbol{\Psi}_3\mathbf{G}\mathbf{Q}\mathbf{Q}^H\mathbf{G}^H\right) \le e, \tag{11f}$$

$$\text{(6b)}. \tag{11g}$$

Furthermore, denote $\boldsymbol{\Psi}_1 = \mathbf{T}_1\mathbf{T}_1^H$, $\boldsymbol{\Psi}_2 = \mathbf{T}_2\mathbf{T}_2^H$, $\boldsymbol{\Psi}_3 = \mathbf{T}_3\mathbf{T}_3^H$, Eq. (11) can be reformulated as

$$\max_{\substack{\mathbf{T}_1\succ\mathbf{0},\mathbf{T}_2\succ\mathbf{0},\\ \mathbf{T}_3\succ\mathbf{0},\mathbf{U},\\ \mathbf{V},\mathbf{W},\mathbf{Q}}} 2\ln|\mathbf{T}_1| - \mathrm{Tr}\left(\mathbf{T}_1\mathbf{T}_1^H\mathbf{U}^H\mathbf{U}\right) - a - b + 2\ln|\mathbf{T}_2| - \sigma_e^{-2}\mathrm{Tr}\left(\mathbf{T}_2\mathbf{T}_2^H\mathbf{V}^H\mathbf{V}\right) - c \tag{12a}$$

$$+2\ln|\mathbf{T}_3| - \sigma_e^2\mathrm{Tr}\left(\mathbf{T}_3\mathbf{T}_3^H\right) - d - e,$$

$$\text{s.t. } \left\|\mathbf{T}_1^H\left(\mathbf{I}-\sigma_b^{-1}\mathbf{U}^H\mathbf{H}\mathbf{W}\right)\right\|_F^2 \le a, \tag{12b}$$

$$\left\|\mathbf{T}_1^H\mathbf{U}^H\mathbf{H}\mathbf{Q}\right\|_F^2 \le \sigma_b^2 b, \tag{12c}$$

$$\left\|\mathbf{T}_2^H\left(\mathbf{I}-\sigma_e^{-1}\mathbf{V}^H\mathbf{G}\mathbf{Q}\right)\right\|_F^2 \le c, \tag{12d}$$

$$\left\|\mathbf{T}_3^H\mathbf{G}\mathbf{W}\right\|_F^2 \le d, \tag{12e}$$

$$\left\|\mathbf{T}_3^H\mathbf{G}\mathbf{Q}\right\|_F^2 \le e, \tag{12f}$$

$$\text{(6b)}. \tag{12g}$$

Eq. (12) is still hard to handle due to the CSI uncertainty. Next, we will introduce the following Nemirovski Lemma to handle the CSI uncertainty. Firstly, we rewrite Eq. (12b) as $\left\|\mathbf{T}_1^H - \sigma_b^{-1}\mathbf{T}_1^H\mathbf{U}^H\left(\bar{\mathbf{H}}+\Delta\mathbf{H}\right)\mathbf{W}\right\|_F^2 \le a$, $\|\Delta\mathbf{H}\|_F \le \chi_H$.

By denoting $\Delta\mathbf{h} = \mathrm{vec}\left(\Delta\mathbf{H}\right)$ and invoking the equation $\mathrm{vec}\left(\mathbf{A}_1\mathbf{A}_2\mathbf{A}_3\right) = \left(\mathbf{A}_3^T\otimes\mathbf{A}_1\right)\mathrm{vec}\left(\mathbf{A}_2\right)$, we obtain the relationship $\left\|\mathbf{t}_1 - \sigma_b^{-1}\mathbf{P}_1\Delta\mathbf{h}\right\|_2^2 \le a$, $\|\Delta\mathbf{h}\|_2 \le \chi_H$, where $\mathbf{t}_1 = \mathrm{vec}\left(\mathbf{X}_1\bar{\mathbf{H}}\mathbf{W} - \mathrm{T}_1^H\right)$, $\mathbf{P}_1 = \mathbf{W}^T\otimes\mathbf{X}_1$ and $\mathbf{X}_1 = \mathbf{T}_1^H\mathbf{U}^H$.

Based on the Schur complement, the above relationship can be reformulated as

$$\begin{bmatrix} a & \left(\mathbf{t}_1-\mathbf{P}\Delta\mathbf{h}\right)^H \\ \mathbf{t}_1-\mathbf{P}\Delta\mathbf{h} & \mathbf{I}\end{bmatrix} \succeq \mathbf{0},\ \|\Delta\mathbf{h}\|_2 \le \chi_H. \tag{13}$$

Furthermore, Eq. (13) can be rewritten as follows

$$\begin{bmatrix} a & \mathbf{t}_1^H \\ \mathbf{t}_1 & \mathbf{I}\end{bmatrix} \succeq \begin{bmatrix}\mathbf{0}\\ \mathbf{P}\end{bmatrix}\Delta\mathbf{h}\left[-1\ \ \mathbf{0}\right] + \begin{bmatrix}-1\\ \mathbf{0}\end{bmatrix}\Delta\mathbf{h}^H\begin{bmatrix}\mathbf{0}\\ \mathbf{P}\end{bmatrix}^H. \tag{14}$$

Next, we will introduce the following Nemirovski Lemma to handle the CSI uncertainty.

Lemma 2 (Nemirovski Lemma) [24, 25]: For a given set of matrices $\mathbf{A} = \mathbf{A}^H$, $\mathbf{B}$ and $\mathbf{C}$, the following LMI is satisfied

$$\mathbf{A} \succeq \mathbf{B}^H\mathbf{X}\mathbf{C} + \mathbf{C}^H\mathbf{X}^H\mathbf{B},\ \|\mathbf{X}\| \le t,$$

if and only if there exists a non-negative real number μ such that

$$\begin{bmatrix}\mathbf{A}-\mu\mathbf{C}^H\mathbf{C} & -t\mathbf{B}^H \\ -t\mathbf{B} & \mu\mathbf{I}\end{bmatrix} \succeq \mathbf{0}.$$

Based on the Nemirovski Lemma, Eq. (14) can be rewritten as the following LMI

$$\begin{bmatrix} a-\lambda_1 & \mathbf{t}_1^H & \mathbf{0} \\ \mathbf{t}_1 & \mathbf{I} & \chi_H \mathbf{P}_1 \\ \mathbf{0} & \chi_H \mathbf{P}_1^H & \lambda_1 \mathbf{I} \end{bmatrix} \succeq \mathbf{0}. \tag{15}$$

where $\lambda_1 \geq 0$ is the introduced auxiliary variables.

Similarly, we denote $\mathbf{t}_2 = \mathrm{vec}(\mathbf{X}_1\bar{\mathbf{H}}\mathbf{Q})$, $\mathbf{P}_2 = \mathbf{Q}^T \otimes \mathbf{X}_1$, $\mathbf{t}_3 = \mathrm{vec}(\mathbf{X}_2\bar{\mathbf{G}}\mathbf{Q} - \mathrm{T}_2^H)$, $\mathbf{P}_3 = \mathbf{Q}^T \otimes \mathbf{X}_2$, $\mathbf{X}_2 = \mathbf{T}_2^H\mathbf{V}^H$, $\mathbf{t}_4 = \mathrm{vec}(\mathbf{T}_3\bar{\mathbf{G}}\mathbf{W})$, $\mathbf{P}_4 = \mathbf{W}^T \otimes \mathbf{T}_3$, $\mathbf{t}_5 = \mathrm{vec}(\mathbf{T}_3\bar{\mathbf{G}}\mathbf{Q})$, $\mathbf{P}_5 = \mathbf{Q}^T \otimes \mathbf{T}_3$, then, the following LMIs can be obtained

$$\begin{bmatrix} \sigma_b^2 b-\lambda_2 & \mathbf{t}_2^H & \mathbf{0} \\ \mathbf{t}_2 & \mathbf{I} & \chi_H \mathbf{P}_2 \\ \mathbf{0} & \chi_H \mathbf{P}_2^H & \lambda_2 \mathbf{I} \end{bmatrix} \succeq \mathbf{0}, \tag{16}$$

$$\begin{bmatrix} c-\lambda_3 & \mathbf{t}_3^H & \mathbf{0} \\ \mathbf{t}_3 & \mathbf{I} & \chi_G \mathbf{P}_3 \\ \mathbf{0} & \chi_G \mathbf{P}_3^H & \lambda_3 \mathbf{I} \end{bmatrix} \succeq \mathbf{0}, \tag{17}$$

$$\begin{bmatrix} d-\lambda_4 & \mathbf{t}_4^H & \mathbf{0} \\ \mathbf{t}_4 & \mathbf{I} & \chi_G \mathbf{P}_4 \\ \mathbf{0} & \chi_G \mathbf{P}_4^H & \lambda_4 \mathbf{I} \end{bmatrix} \succeq \mathbf{0}, \tag{18}$$

$$\begin{bmatrix} e-\lambda_5 & \mathbf{t}_5^H & \mathbf{0} \\ \mathbf{t}_5 & \mathbf{I} & \chi_G \mathbf{P}_5 \\ \mathbf{0} & \chi_G \mathbf{P}_5^H & \lambda_5 \mathbf{I} \end{bmatrix} \succeq \mathbf{0}, \tag{19}$$

where $\{\lambda_2 \geq 0, \cdots, \lambda_5 \geq 0\}$ are introduced auxiliary variables.

Bases on these above operations, we obtain the following problem

$$\max_{\substack{\mathbf{T}_1\succ\mathbf{0},\mathbf{T}_2\succ\mathbf{0},\\ \mathbf{T}_3\succ\mathbf{0},\mathbf{U},\\ \mathbf{V},\mathbf{W},\mathbf{Q}}} \; 2\ln|\mathbf{T}_1| - \mathrm{Tr}\left(\mathbf{T}_1\mathbf{T}_1^H\mathbf{U}^H\mathbf{U}\right) - a - b + 2\ln|\mathbf{T}_2| - \sigma_e^{-2}\mathrm{Tr}\left(\mathbf{T}_2\mathbf{T}_2^H\mathbf{V}^H\mathbf{V}\right)$$
$$- c + 2\ln|\mathbf{T}_3| - \sigma_e^2\mathrm{Tr}\left(\mathbf{T}_3\mathbf{T}_3^H\right) - d - e, \tag{20a}$$

$$\text{s.t.} \quad (6b), (15), (16), (17), (18), (19). \tag{20b}$$

To this end, we turn Eq. (6) into an equivalent problem in Eq. (12). Eq. (12) is still non-convex w.r.t all these optimization variables, but is convex w.r.t given variables when other variables are fixed. Specifically, these variables can be divided into three groups: $\{\mathbf{W}, \mathbf{Q}\}$, $\{\mathbf{U}, \mathbf{V}\}$, and $\{\mathbf{T}_1, \mathbf{T}_2, \mathbf{T}_3\}$. Then, Eq. (12) can be decoupled into four subproblems w.r.t these variables. Both these subproblems can be effectively solved by the convex optimization tool CVX [28], and the optimal solution to Eq. (6) can be achieved in an alternating method.

4. OUTAGE SECRECY DESIGN

In this section, we will handle the outage secrecy design. As discussed in the above, we find that the OCSRM problem is non-convex due to the constraints in Eq. (7b). Hence, in the following, in order to solve the OCSRM problem, we propose an effective way to convert the non-convex constraints.

Based on Equation (1) and denoting $\boldsymbol{\mathcal{W}} = \mathbf{W}\mathbf{W}^H$, we obtain the following relationship

$$-\ln\left|\mathbf{I} + \sigma_b^{-2}\mathbf{H}\boldsymbol{\mathcal{W}}\mathbf{H}^H\right| = \max_{\mathbf{S}_b\succeq\mathbf{0}} f\left(\mathbf{S}_b, \mathbf{I} + \sigma_b^{-2}\mathbf{H}\boldsymbol{\mathcal{W}}\mathbf{H}^H\right), \tag{21a}$$

$$-\ln\left|\mathbf{I} + \sigma_e^{-2}\mathbf{G}\left(\boldsymbol{\mathcal{W}} + \boldsymbol{\Sigma}\right)\mathbf{G}^H\right| = \max_{\mathbf{S}_e\succeq\mathbf{0}} f\left(\mathbf{S}_e, \mathbf{I} + \sigma_e^{-2}\mathbf{G}\left(\boldsymbol{\mathcal{W}} + \boldsymbol{\Sigma}\right)\mathbf{G}^H\right), \tag{21b}$$

where $\mathbf{S}_b$ and $\mathbf{S}_e$ are introduced auxiliary variables.

In addition, at low signal-to-noise ratio (SNR) region, we invoke the following SNR approximation method [23],

$$\ln\left|\mathbf{I}+\sigma_b^{-2}\mathbf{H}\left(\boldsymbol{\mathcal{W}}+\boldsymbol{\Sigma}\right)\mathbf{H}^H\right|=\sigma_b^{-2}\mathrm{Tr}\left(\mathbf{H}\left(\boldsymbol{\mathcal{W}}+\boldsymbol{\Sigma}\right)\mathbf{H}^H\right), \tag{22a}$$

$$\ln\left|\mathbf{I}+\sigma_e^{-2}\mathbf{G}\boldsymbol{\mathcal{W}}\mathbf{G}^H\right|=\sigma_e^{-2}\mathrm{Tr}\left(\mathbf{G}\boldsymbol{\mathcal{W}}\mathbf{G}^H\right). \tag{22b}$$

By substituting Eqs. (21) and (22) into Eq. (5), we obtain the following probability constraint

$$\begin{aligned}\Pr\Big\{&\sigma_b^{-2}\mathrm{Tr}\left(\mathbf{H}\left(\boldsymbol{\mathcal{W}}+\boldsymbol{\Sigma}\right)\mathbf{H}^H\right)+\sigma_e^{-2}\mathrm{Tr}\left(\mathbf{G}\boldsymbol{\mathcal{W}}\mathbf{G}^H\right)\\&+\max_{\mathbf{S}_e\succeq\mathbf{0}}f\left(\mathbf{S}_e,\mathbf{I}+\sigma_e^{-2}\mathbf{G}\left(\boldsymbol{\mathcal{W}}+\boldsymbol{\Sigma}\right)\mathbf{G}^H\right)\\&+\max_{\mathbf{S}_b\succeq\mathbf{0}}f\left(\mathbf{S}_b,\mathbf{I}+\sigma_b^{-2}\mathbf{H}\boldsymbol{\mathcal{W}}\mathbf{H}^H\right)\geq R\Big\}\geq 1-\rho,\end{aligned} \tag{23}$$

which can be further safely approximated as

$$\begin{aligned}\Pr\Big\{&\sigma_b^{-2}\mathrm{Tr}\left(\mathbf{H}\left(\boldsymbol{\mathcal{W}}+\boldsymbol{\Sigma}\right)\mathbf{H}^H\right)+\sigma_e^{-2}\mathrm{Tr}\left(\mathbf{G}\boldsymbol{\mathcal{W}}\mathbf{G}^H\right)\\&+f\left(\mathbf{S}_e,\mathbf{I}+\sigma_e^{-2}\mathbf{G}\left(\boldsymbol{\mathcal{W}}+\boldsymbol{\Sigma}\right)\mathbf{G}^H\right)\\&+f\left(\mathbf{S}_b,\mathbf{I}+\sigma_b^{-2}\mathbf{H}\boldsymbol{\mathcal{W}}\mathbf{H}^H\right)\geq R\Big\}\geq 1-\rho.\end{aligned} \tag{24}$$

Next, we turn channel matrices $\mathbf{H}$ and $\mathbf{G}$ into the following form $\mathbf{h}=\bar{\mathbf{h}}+\mathbf{C}_h^{1/2}\mathbf{v}_h$ where $\mathbf{h}=\mathrm{vec}\left(\mathbf{H}\right)$ and $\bar{\mathbf{h}}=\mathrm{vec}\left(\bar{\mathbf{H}}\right)$, $\mathbf{v}_h\sim\mathcal{CN}\left(\mathbf{0},\mathbf{I}\right)$, $\mathbf{g}=\bar{\mathbf{g}}+\mathbf{C}_g^{1/2}\mathbf{v}_g$. Similarly, $\mathbf{g}=\mathrm{vec}\left(\mathbf{G}\right)$, $\bar{\mathbf{g}}=\mathrm{vec}\left(\bar{\mathbf{G}}\right)$, $\mathbf{v}_g\sim\mathcal{CN}\left(\mathbf{0},\mathbf{I}\right)$.

By invoking the equations $\mathrm{Tr}\left(\mathbf{ABC}^H\right)=\mathrm{vec}(\mathbf{C})^H\left(\mathbf{B}^T\otimes\mathbf{I}\right)\mathrm{vec}\left(\mathbf{A}\right)$ and $\mathrm{Tr}\left(\mathbf{A}^H\mathbf{BCD}\right)=\mathrm{vec}(\mathbf{A})^H\left(\mathbf{D}^T\otimes\mathbf{B}\right)\mathrm{vec}\left(\mathbf{C}\right)$, Eq. (24) can be rewritten as the following equation

$$\begin{aligned}\Pr\Big\{&\left[\mathbf{v}_h^H\ \mathbf{v}_g^H\right]\begin{bmatrix}\mathbf{C}_h^{1/2}\boldsymbol{\Theta}_1\mathbf{C}_h^{1/2} & \mathbf{0}\\ \mathbf{0} & \mathbf{C}_g^{1/2}\boldsymbol{\Theta}_2\mathbf{C}_g^{1/2}\end{bmatrix}\begin{bmatrix}\mathbf{v}_h\\ \mathbf{v}_g\end{bmatrix}\\&+2\Re\left\{\left[\mathbf{v}_h^H\ \mathbf{v}_g^H\right]\begin{bmatrix}\mathbf{C}_h^{1/2}\boldsymbol{\Theta}_1 & \mathbf{0}\\ \mathbf{0} & \mathbf{C}_g^{1/2}\boldsymbol{\Theta}_2\end{bmatrix}\begin{bmatrix}\mathbf{h}\\ \mathbf{g}\end{bmatrix}\right\}\\&+\left[\mathbf{h}^H\ \mathbf{g}^H\right]\begin{bmatrix}\boldsymbol{\Theta}_1 & \mathbf{0}\\ \mathbf{0} & \boldsymbol{\Theta}_2\end{bmatrix}\begin{bmatrix}\mathbf{h}\\ \mathbf{g}\end{bmatrix}+\varphi\geq 0\Big\}\geq 1-\rho,\end{aligned} \tag{25}$$

where $\boldsymbol{\Theta}_1=\sigma_b^{-2}\left(\left(\boldsymbol{\mathcal{W}}^T+\boldsymbol{\Sigma}^T\right)\otimes\mathbf{I}-\boldsymbol{\mathcal{W}}^T\otimes\mathbf{S}_b\right)$, $\boldsymbol{\Theta}_2=\sigma_e^{-2}\left(\boldsymbol{\mathcal{W}}^T\otimes\mathbf{I}-\left(\boldsymbol{\mathcal{W}}^T+\boldsymbol{\Sigma}^T\right)\otimes\mathbf{S}_e\right)$ and $\varphi=-\mathrm{Tr}\left(\mathbf{S}_b\right)+\ln\left|\mathbf{S}_b\right|+N_b-\mathrm{Tr}\left(\mathbf{S}_e\right)+\ln\left|\mathbf{S}_e\right|+N_e-R$.

Next, we will handle the CSI uncertainty based on the following BTI.

Lemma 2 [26] (BTI): For any $(\mathbf{A},\mathbf{u},c)\in\mathbb{H}^N\times\mathbb{C}^N\times\mathbb{R}$, $\mathbf{v}\sim\mathcal{CN}\left(\mathbf{0},\mathbf{I}\right)$ and $\beta\in(0,1]$, the following inequalities hold:

$$\begin{aligned}&\Pr{}_{\mathbf{v}}\left\{\mathbf{v}^H\mathbf{A}\mathbf{v}+2\Re\left\{\mathbf{v}^H\mathbf{u}\right\}+c\geq 0\right\}\geq 1-\beta\\&\Leftarrow\begin{cases}\mathrm{Tr}\left(\mathbf{A}\right)-\sqrt{-2\ln\left(\beta\right)}\mathrm{x}+\ln\left(\beta\right)\mathrm{y}+\mathrm{c}\geq 0,\\ \left\|\begin{bmatrix}\mathrm{vec}\left(\mathbf{A}\right)\\ \sqrt{2}\mathbf{u}\end{bmatrix}\right\|\leq x,\\ y\mathbf{I}+\mathbf{A}\succeq\mathbf{0},y\geq 0,\end{cases}\end{aligned}$$

where x and y are slack variables. Moreover, BTI is convex w.r.t all the variables $(\mathbf{A},\mathbf{u},c,x,y)$.

Based on BTI and denoting $\mathbf{v}\triangleq\left[\mathbf{v}_h^H\ \mathbf{v}_h^H\right]^H$,

$$\mathbf{A}\triangleq\begin{bmatrix}\mathbf{C}_h^{1/2}\boldsymbol{\Theta}_1\mathbf{C}_h^{1/2} & \mathbf{0}\\ \mathbf{0} & \mathbf{C}_g^{1/2}\boldsymbol{\Theta}_2\mathbf{C}_g^{1/2}\end{bmatrix}, \tag{26}$$

$$\mathbf{u}\triangleq\begin{bmatrix}\mathbf{C}_h^{1/2}\boldsymbol{\Theta}_1 & \mathbf{0}\\ \mathbf{0} & \mathbf{C}_g^{1/2}\boldsymbol{\Theta}_2\end{bmatrix}\begin{bmatrix}\mathbf{h}\\ \mathbf{g}\end{bmatrix}, \tag{27}$$

$$c \triangleq \left[\mathbf{h}^H \ \mathbf{g}^H\right] \begin{bmatrix} \mathbf{\Theta}_1 & \mathbf{0} \\ \mathbf{0} & \mathbf{\Theta}_2 \end{bmatrix} \begin{bmatrix} \mathbf{h} \\ \mathbf{g} \end{bmatrix} + \varphi, \tag{28}$$

we obtain the following relationship

$$\begin{cases} \mathrm{Tr}\,(\mathbf{A}) - \sqrt{-2\ln(\rho)}x + \ln(\rho)\,y + c \geq 0, \\ \left\| \begin{matrix} \mathrm{vec}\,(\mathbf{A}) \\ \sqrt{2}\mathbf{u} \end{matrix} \right\|_2 \leq x, \\ y\mathbf{I} + \mathbf{A} \succeq \mathbf{0}. \end{cases} \tag{29}$$

To this end, we turn Eq. (25) into a solvable reformulation.

In addition, to reduce the computation complexity of the BTI method, we propose to use the following LDI method.

Lemma 3 [27] (LDI): Let $\mathbf{x} \sim \mathcal{CN}(\mathbf{0}, \mathbf{I})$, and $\mathbf{A} \in \mathbb{H}^{n\times n}$, $\mathbf{r} \in \mathbb{C}^{n\times 1}$ are given. Then, for any $v > \frac{1}{\sqrt{2}}$ and $\zeta > 0$, we have

$$\begin{aligned} &\Pr\left\{\mathbf{x}^H\mathbf{A}\mathbf{x} + 2\Re\left\{\mathbf{x}^H\mathbf{r}\right\} \leq \mathrm{Tr}\,(\mathbf{A}) - \zeta\right\} \\ &\leq \begin{cases} \exp\left(-\dfrac{\zeta^2}{4T^2}\right) & 0 < \zeta \leq 2\bar{v}vT, \\ \exp\left(-\dfrac{\bar{v}v\zeta}{T} + (\bar{v}v)^2\right) & \zeta > 2\bar{v}vT, \end{cases} \end{aligned}$$

where $\bar{v} = 1 - \frac{1}{2v^2}$ and $T = v\|\mathbf{A}\|_F + \frac{1}{\sqrt{2}}\|\mathbf{r}\|$. Similarly with BTI, LDI is also convex w.r.t all the variables $(\mathbf{A}, \mathbf{u}, c, x, y)$.

Based on LDI, we transform Eq. (25) into the following relationship

$$\begin{cases} \mathrm{Tr}\,(\mathbf{A}) + c \geq 2\sqrt{-\ln(\rho)}\,(x+y)\,, \\ \|\mathbf{u}\|_2 \leq \sqrt{2}x, \\ v\|\mathbf{A}\|_F \leq y, \end{cases} \tag{30}$$

where v is the solution of the following equation $\bar{v}v = (1 - 1/2v^2)v = \sqrt{-\ln(\rho)}$.

For both BTI and LDI based methods, Eqs. (29) and (30) are still non-convex w.r.t all these optimization variables, but are convex w.r.t certain variables when other variables are fixed. Specifically, these variables can be divided into two groups: $\{\mathcal{W}, \mathbf{\Sigma}\}$ and $\{\mathbf{S}_b, \mathbf{S}_e\}$. Then, Eq. (24) can be decoupled into four subproblems w.r.t these variables. Both these subproblems can be effectively solved by the

Table 1. Complexity analysis of BTI and LDI methods.

problems	Complexity Order ($\ln(1/\varepsilon)\sqrt{\beta(\mathcal{K})}\mathcal{C}$, ε denotes the accuracy requirement.)
subproblem 1 with BTI	$\beta(\mathcal{K}) = (2 + N_r + N_e)\,N_t + 4$, $\mathcal{C} = n^3 + n\left[(N_r+N_e)^3N_t^3 + 2N_t^3 + 2\right]$ $+n^2\left[(N_r+N_e)^2N_t^2 + 2N_t^2 + 2\right] + nN_t^2(N_r+N_e)^2(N_tN_r + N_tN_e + 1)^2$, and $n = \mathcal{O}\left(2N_t^2\right)$.
subproblem 2 with BTI	$\beta(\mathcal{K}) = (2 + N_r + N_e)\,N_t + 2$, $\mathcal{C} = n^3 + n\left[(N_r+N_e)^3N_t^3 + 2N_t^3\right]$ $+n^2\left[(N_r+N_e)^2N_t^2 + 2N_t^2\right] + nN_t^2(N_r+N_e)^2(N_tN_r + N_tN_e + 1)^2$, and $n = \mathcal{O}\left(N_r^2 + N_e^2\right)$.
subproblem 1 with LDI	$\beta(\mathcal{K}) = 2N_t + 5$, $\mathcal{C} = n^3 + n\left(2N_t^2+1\right)^3 + n^2\left(2N_t^2+1\right)^2 +$ $nN_t^4(N_r+N_e)^4 + nN_t^2(N_r+N_e)^2$, and $n = \mathcal{O}\left(2N_t^2\right)$.
subproblem 2 with LDI	$\beta(\mathcal{K}) = 2N_t + 4$, $\mathcal{C} = n^3 + 2nN_t^6 + 2n^2N_t^4 + nN_t^4(N_r+N_e)^4$ $+nN_t^2(N_r+N_e)^2$, and $n = \mathcal{O}\left(N_r^2 + N_e^2\right)$.

convex optimization tool CVX [28], and the optimal solution to Eq. (6) can be achieved in an alternating method.

Via a similar way to that in [27], we obtain the complexity comparison between BTI and LDI methods, which are shown in Table 1. From the comparison, we observe that the LDI method achieves lower complexity than the BTI method.

5. SIMULATION RESULTS

In this section, we evaluate the performance of our proposed design through Monte Carlo simulations. The simulation settings are assumed as follows: $P_s = 10\,\text{dBW}$, $\sigma_b^2 = \sigma_e^2 = 10^{-4}$. Each element of $\bar{\mathbf{H}}$ and $\bar{\mathbf{G}}$ is randomly generated by $\mathcal{CN}(0, 10^{-4})$, and the channel uncertainties are $\chi_H^2 = \chi_G^2 = 2 \times 10^{-6}$ for bounded uncertainty and $\mathbf{C}_H = \mathbf{C}_G = 2 \times 10^{-6}$ for the outage case, respectively. The outage probability is $\rho = 0.05$. For the worst case design, we compare our algorithm with the following methods: 1) The case of perfect CSI, which can be seen as the upper bound of our proposed design; 2) The no AN method, e.g., setting $\mathbf{\Sigma} = \mathbf{0}$ while only optimizing $\mathbf{W}$; 3) The SCA based method in [16]; 4) The MM based method in [13]. The five methods are denoted as "the proposed method", "the perfect CSI case", "the no AN method", "the SCA based method", and "the MM based method", respectively. On the other hand, for the outage case design, we compare our BTI and LDI methods with the following methods: 1) The case of perfect CSI; 2) The no AN method; 3) The MM based method. The five methods are denoted as "the BTI method", "the LDI method", "the perfect CSI case", "the no AN method", and "the MM based method", respectively.

5.1. Worst Case Performance

Firstly, in Fig. 2, we show the convergency of our proposed AO method with random channel realization. From this figure, we can see that for different channel conditions, the proposed method can always convergent in limited AO numbers.

Secondly, in Fig. 3, we show the worst case secrecy rate R_{worst} versus the source transmit power P_s. From this figure, we can see that our proposed method achieves better performance than the other methods. In addition, the performance gaps among the four methods with the perfect CSI case become larger with the increase of P_s, while the SCA method tends to decrease in respectively high P_s region.

Furthermore, in Fig. 4, we show the worst case secrecy rate R_{worst} versus the channel uncertainty level. The proposed method achieves better performance than other methods. For all these methods,

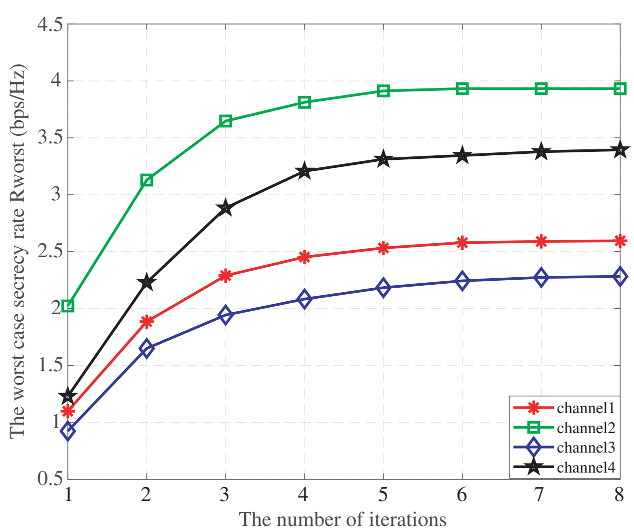

Figure 2. The convergency versus the iterative numbers.

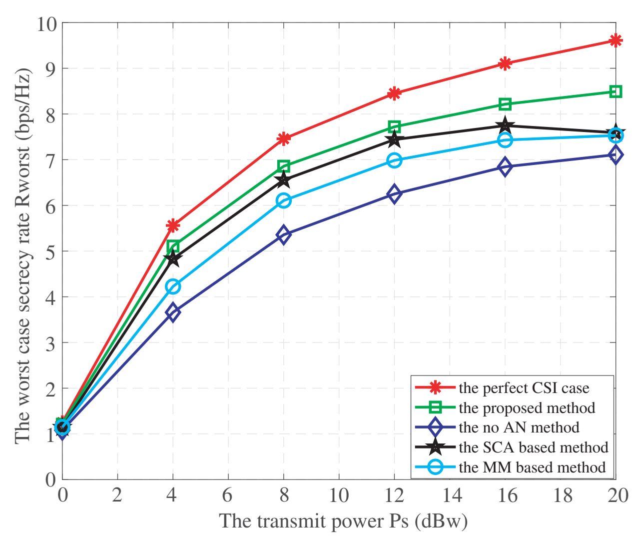

Figure 3. The worst case secrecy rate versus the source transmit power.

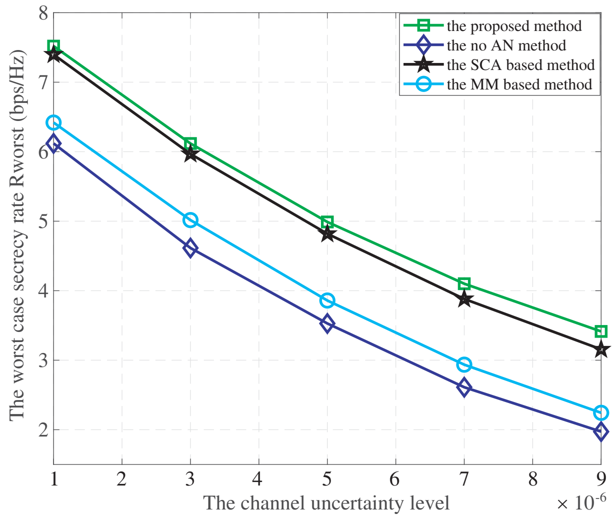

Figure 4. The worst case secrecy rate versus the uncertainty level.

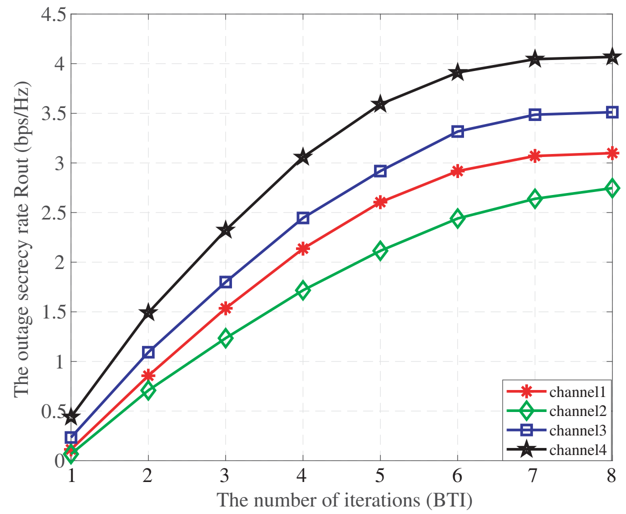

Figure 5. The BTI convergency versus the iterative numbers.

R_{worst} tends to decrease with the increase of the channel uncertainty level, which shows the impact of the channel uncertainty on the secrecy performance.

5.2. Outage Secrecy Performance

Firstly, in Fig. 5 and Fig. 6, we show the convergency of the proposed BTI and LDI methods with random channel realization. Similarly with the previous AO method, both the BTI and LDI methods can be convergent in limited AO numbers.

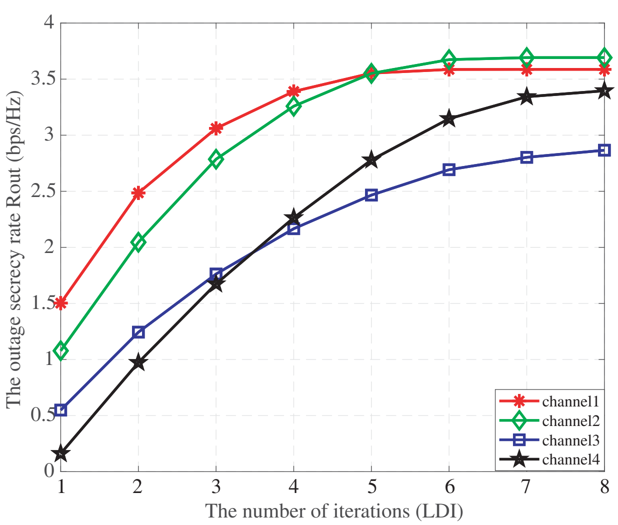

Figure 6. The LDI convergency versus the iterative numbers.

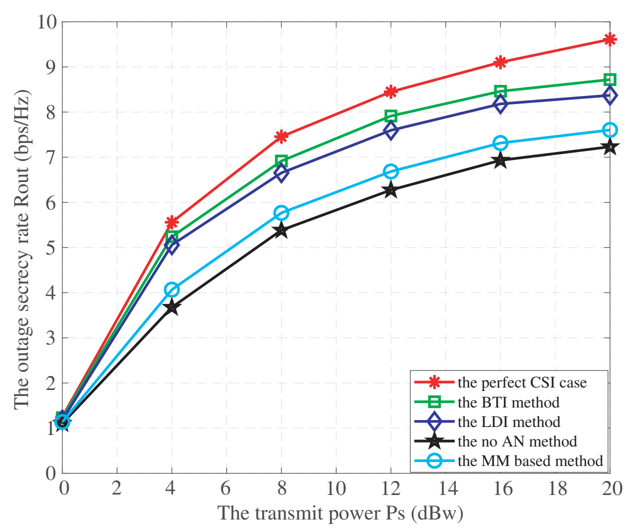

Figure 7. The outage secrecy rate versus the source transmit power.

Secondly, in Fig. 7, we show the outage secrecy rate R_{out} versus the source transmit power P_s. From this figure, we can see that our proposed method achieves better performance than the other methods. In addition, the no AN design suffers from the worst performance, which suggests the importance of AN in resistance of the channel uncertainty.

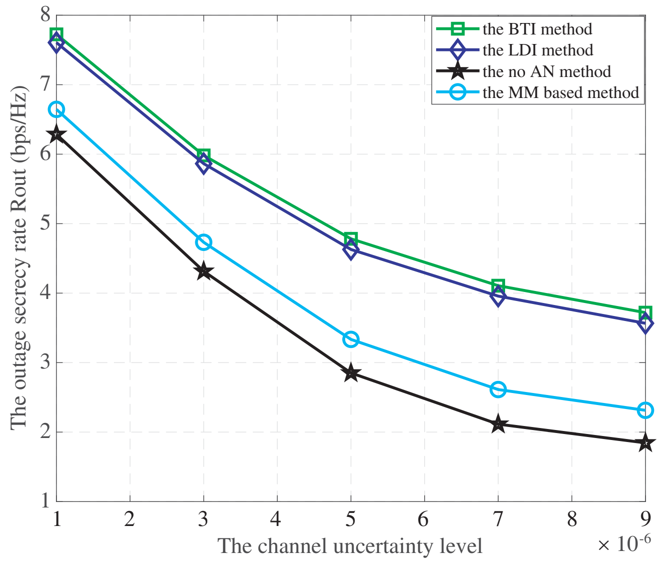

Figure 8. The outage secrecy rate versus the uncertainty level.

Lastly, in Fig. 8, we show the outage secrecy rate R_{out} versus channel uncertainty level. From this figure, we can see that the gap between BTI and LDI methods is tiny. However, the performance loss for the no AN method is quite large, which suggests the necessity of AN again.

6. CONCLUSION

In this paper, we have investigated both WC and OC robust secrecy designs in MIMO wiretap WSNs. To solve the WC design, we propose to linearize log-det terms in the secrecy rate expression. After linearization, we tackle the CSI uncertainty based on epigraph reformulation and the Nemirovski lemma. Then, an AO algorithm is designed to solve the reformulated problem. Furthermore, to solve the OC design, we transform the probabilistic constraint into tractable approximation by the BTI and LDI. Numerical results are provided to demonstrate the performance of the proposed scheme.

7. FUNDING

The author(s) disclosed receipt of the following financial support for the research, authorship, and/or publication of this article: This work was part supported by the National Natural Science Foundation of China under Grant No. 61673108, part supported by the Colleges and Universities Natural Science Foundation in Jiangsu Province under contracts No. 18KJB510010 and No. 19KJA110002, part supported by the industry-university-research cooperation project of Jiangsu province under Grant No. BY2018282, part supported by the Open Project Program of the Key Laboratory of Underwater Acoustic Signal Processing, Ministry of Education, China under contracts No. UASP1801, and part supported by the Fundamental Research Funds for the Central Universities under contracts No. 2242016K30013.

REFERENCES

1. Choi, K. W., L. Ginting, P. A. Rosyady, A. A. Aziz, and D. I. Kim, "Wireless-powered sensor networks: How to realize," *IEEE Trans. Wireless Commun.*, Vol. 16, No. 1, 221–234, Jan. 2017.
2. Ruan, T., Z. Chew, and M. Zhu, "Energy-aware approaches for energy harvesting powered wireless sensor nodes," *IEEE Sensor Journal*, Vol. 17, No. 7, 2165–2173, Apr. 2017.

3. Wu, J., K. Ota, M. Dong, and C. Li, "A hierarchical security framework for defending against sophisticated attacks on wireless sensor networks in smart cities," *IEEE Access*, Vol. 4, 416–424, Jan. 2016.
4. Deng, Y., L. Wang, M. Elkashlan, A. Nallanathan, and R.K. Mallik, "Physical layer security in three-tier wireless sensor networks: A stochastic geometry approach," *IEEE Trans. Inf. Forensics Security*, Vol. 11, No. 6, 1128–1138, Jan. 2016.
5. Liu, Y., H.-H. Chen, and L. Wang, "Physical layer security for next generation wireless networks: Theories, technologies, and challenges," *IEEE Commun. Surveys Tutorials*, Vol. 19, No. 1, 347–376, First Quarter, 2017.
6. Khisti, A. and G. W. Wornell, "Secure transmission with multiple antennas — Part II: The MIMOME wiretap channel," *IEEE Trans. Inf. Theory*, Vol. 56, No. 11, 5515–5532, Nov. 2010.
7. Oggier, F. and B. Hassibi, "The secrecy capacity of the MIMO wiretap channel," *IEEE Trans. Inf. Theory*, Vol. 57, No. 8, 4961–4972, Aug. 2011.
8. Li, Q., M. Hong, H.-T. Wai, Y.-F. Liu, W.-K. Ma, and Z.-Q. Luo, "Transmit solutions for MIMO wiretap channels using alternating optimization," *IEEE J. Sel. Areas Commun.*, Vol. 31, No. 9, 1714–1727, Sep. 2013.
9. Fakoorian, S. A. A. and A. L. Swindlehurst, "Full rank solutions for the MIMO Gaussian wiretap channel with an average power constraint," *IEEE Trans. Signal Process.*, Vol. 61, No. 10, 2620–2631, May 2013.
10. Loyka, S. and C. D. Charalambous, "An algorithm for global maximization of secrecy rates in gaussian MIMO wiretap channels," *IEEE Trans. Commun.*, Vol. 63, No. 6, 2288–2299, Jan. 2015.
11. Shi, Q.-J., W.-Q. Xu, J.-S. Wu, E.-B. Song, and Y.-M. Wang, "Secure beamforming for MIMO broadcasting with wireless information and power transfer," *IEEE Trans. Wireless Commun.*, Vol. 14, No. 5, 2841–2853, May 2015.
12. Lee, H., C. Song, J. Moon, and I. Lee, "Precoder designs for MIMO Gaussian multiple access wiretap channels," *IEEE Trans. Veh. Tech.*, Vol. 66, No. 9, 8563–8568, Sep. 2017.
13. Masood, M., A. Chrayeb, P. Babu, I. Khalil, and M. Hasna, "A minorization-maximization algorithm for maximizing the secrecy rate of MIMOME wiretap channel," *IEEE Commun. Lett.*, Vol. 21, No. 3, 520–523, Mar. 2017.
14. Cumanan, K., Z. Ding, B. Sharif, G. Y. Tian, and K. K. Leung, "Secrecy rate optimizations for a MIMO secrecy channel with a multiple-antenna eavesdropper," *IEEE Trans. Veh. Tech.*, Vol. 63, No. 4, 1678–1690, May 2014.
15. Chu, Z., K. Cumanan, Z. Ding, M. Johnston, and S. Y. Le Goff, "Secrecy rate optimizations for a MIMO secrecy channel with a cooperative jammer," *IEEE Trans. Veh. Tech.*, Vol. 64, No. 5, 1833–1847, May 2015.
16. Wang, S.-H. and B.-Y. Wang, "Robust secure transmit design in MIMO channels with simultaneous wireless and information power," *IEEE Signal Process. Lett.*, Vol. 22, No. 11, 2147–2151, Nov. 2015.
17. Zhu, Z., Z. Chu, N. Wang, S. Huang, Z. Wang, and I. Lee, "Beamforming and power splitting designs for AN-aided secure multi-user MIMO SWIPT systems," *IEEE Trans. Inf. Forensics Security*, Vol. 12, No. 12, 2861–2874, Dec. 2017.
18. Jiang, M., Y. Li, Q. Zhang, Q. Li, and J. Qin, "Robust secure beamforming in MIMO wiretap channels with deterministically bounded channel errors," *IEEE Trans. Veh. Tech.*, Vol. 67, No. 10, 9775–9784, Oct. 2018.
19. Li, Q., W.-K. Ma, and A. M. Cho, "A safe approximation approach to secrecy outage design for MIMO wiretap channels," *IEEE Signal Process. Lett.*, Vol. 21, No. 1, 118–121, Jun. 2014.
20. Chu, Z., K. Cumanan, Z. Ding, M. Johnston, and S. L. Goff, "Robust outage secrecy rate optimizations for a MIMO secrecy channel," *IEEE Wireless Commun. Lett.*, Vol. 4, No. 1, 86–89, Jun. 2015.
21. Wu, W. and B. Wang, "Efficient transmission solutions for MIMO wiretap channels with SWIPT," *IEEE Commun. Lett.*, Vol. 19, No. 9, 1548–1551, Sep. 2015.

22. Khandaker, M. R. A. and K.-K. Wong, "Robust secrecy beamforming for MIMO SWIPT with probabilistic constraint," *Proc. IEEE Globecom Workshops*, 1–6, Dec. 2016.
23. Yuan, Y. and Z. Ding, "Outage constrained secrecy rate maximization design with SWIPT in MIMO-CR systems," *IEEE Trans. Veh. Tech.*, Vol. 67, No. 6, 5475–5480, Jun. 2018.
24. Eldar, Y. C., A. Ben-Tal, and A. Nemirovski, "Robust mean-squared error estimation in the presence of model uncertainties," *IEEE Trans. Signal Process.*, Vol. 53, No. 1, 168–181, Jan. 2005.
25. Ben-Tal, A., L. E. Ghaoui, and A. Nemirovski, *Robust Optimization*, Princeton Univ. Press, Princeton, NJ, USA, 2009.
26. Bechar, I., "A Bernstein-type inequality for stochastic processes of quadratic forms of Gaussian variables," avaiable online at http://arxiv.org/abs/0909.3595, Sep. 2009.
27. Wang, K.-Y., A. M.-C. So, T.-H. Chang, W.-K. Ma, and C.-Y. Chi, "Outage constrained robust transmit optimization for multiuser MISO downlinks: Tractable approximations by conic optimization," *IEEE Trans. Signal Process.*, Vol. 62, No. 21, 5690–5705, Nov. 2014.
28. Grant, M. and S. Boyd, CVX: Matlab software for disciplined convex programming, version 1.21. Accessed on Apr. 2011. [Online]. Available: http://cvxr.com/cvx.